Turkish Journal of Electrical Engineering & Computer Sciences

http://journals.tubitak.gov.tr/elektrik/

Research Article

Turk J Elec Eng & Comp Sci
(2017) 25: 4805 – 4817

doi:10.3906/elk-1705-92

A probabilistic scenario-based framework for solving stochastic dynamic economic emission dispatch with unit commitment

Yachao ZHANG[1], Kaipei LIU[1,*], Xiaobing LIAO[1], Liang QIN[1], Xueli AN[2]
[1]School of Electrical Engineering, Wuhan University, Wuhan, P.R. China
[2]China Institute of Water Resources and Hydropower Research, Beijing, P.R. China

Received: 07.05.2017 • **Accepted/Published Online:** 21.08.2017 • **Final Version:** 03.12.2017

Abstract: This paper establishes a probabilistic scenario-based framework for the stochastic dynamic economic emission dispatch with unit commitment (SDEED-UC) problem, by considering wind power integration. The scenario generation and reduction method are implemented to describe wind power uncertainty. Accordingly, each wind power scenario is analyzed separately to determine the on/off status of the units. As for a predetermined significance level, the UC scheduling solution can be obtained with a probabilistic point of view, considering all the original scenarios. Then the SDEED problem is converted into a number of deterministic scheduling problems. For each scenario in the reduced set, an enhanced multiobjective particle swarm optimization algorithm is proposed to produce the Pareto optimal solutions. The practicability and performance of the proposed approach are illustrated through a case study, and the results are compared with the existing multiobjective evolutionary algorithms.

Key words: Wind power, unit commitment, dynamic economic emission dispatch, probabilistic analysis method, enhanced multiobjective particle swarm optimization

1. Introduction

The intermittency and uncertainty of wind power generation have posed new challenges to power system optimal dispatch with high integration of wind energy. The unit commitment (UC) problem, considering wind power uncertainty, has been studied by many researchers [1]. Additionally, the stochastic programming method [2,3] and the robust optimization model [4,5] have been studied.

On the other hand, different evolutionary algorithms have been implemented for the dynamic economic dispatch problem [6,7]. The pollutant emission caused by thermal plants was not considered in the above studies. However, the dynamic economic emission dispatch (DEED) problem has received much attention [8]. The economic emission dispatch problem was converted to single-objective by price penalty and weighted factors [9,10]. Since DEED is a multiobjective optimization problem (MOOP), the classic multiobjective evolutionary algorithms (MOEAs) include nondominated sorting genetic algorithm (NSGA-II) [11], multiobjective particle swarm optimization (MOPSO) [12], and multiobjective evolutionary algorithm based on decomposition (MOEA/D) [13]. Many researchers have studied different MOEAs to solve DEED with wind power integration, such as modified particle swarm optimization [14], gravitational search based on a nondominated sorting genetic approach [15], normalized normal constraint algorithm [16], and summation-based MOEA [17]. However, the

*Correspondence: kaipeiliu@gmail.com

DEED problem with UC has rarely been reported in the existing research. Although it has been presented, the stochastic characteristics of wind power and the ramp-up/down capacity limits of units have not been considered [18].

Considering the current research, the purpose of this work was to establish a comprehensive framework to solve the stochastic dynamic economic emission dispatch with unit commitment (SDEED-UC) problem, integrated with wind power. The Pareto optimal solutions by the proposed enhanced MOPSO are compared to the results of the other algorithms, and the best compromise solutions under different significance levels are analyzed across the aspects of economic, emission and reliability.

2. Problem formulation

2.1. Economic objective function

The generation cost of thermal plants can be expressed as

$$\text{Min } F = \sum_{s=1}^{S} Pr(s) \cdot f_{\cos t}^{s} = \sum_{s=1}^{S} Pr(s) \cdot \left\{ \sum_{j=1}^{T} \sum_{i=1}^{N} \left[SC_i \cdot (1 - u_{i,j-1}) \cdot u_{i,j} + u_{i,j} \cdot f_i(P_{i,j}^{s}) \right] \right\}, \tag{1}$$

where

$$SC_i = \begin{cases} SC_i^{hot} : MDT_i \le TOFF_{i,j} \le MDT_i + T_i^{cold} \\ SC_i^{cold} : TOFF_{i,j} > MDT_i + T_i^{cold} \end{cases} \tag{2}$$

$$f_i(P_{i,j}^{s}) = a_i + b_i P_{i,j}^{s} + c_i (P_{i,j}^{s})^2, \tag{3}$$

where a_i, b_i, and c_i are the fuel cost coefficients of unit i.

2.2. Environmental objective function

The pollution emission caused by thermal plants can be expressed as

$$\text{Min } E = \sum_{s=1}^{S} Pr(s) \cdot f_{emi}^{s} = \sum_{s=1}^{S} Pr(s) \cdot \left\{ \sum_{j=1}^{T} \sum_{i=1}^{N} \left[u_{i,j} \cdot (\alpha_i + \beta_i \cdot P_{i,j}^{s} + \gamma_i \cdot (P_{i,j}^{s})^2 + \eta_i \exp(\delta_i \cdot P_{i,j}^{s})) \right] \right\}, \tag{4}$$

where α_i, β_i, γ_i, η_i, and δ_i are the emission coefficients of unit i.

2.3. Constraints

1) System power balance:

$$\sum_{i=1}^{N} u_{i,j} \cdot P_{i,j}^{s} + W_j^{s} = P_{D,j} \tag{5}$$

2) System up/down spinning reserve constraints:

$$\begin{cases} \sum\limits_{i=1}^{N} u_{i,j} \cdot P_{i,\max} \ge (1 + \eta) \cdot P_{D,j} - (1 - us) \cdot W_j^{s} \\ \sum\limits_{i=1}^{N} u_{i,j} \cdot P_{i,\min} \le P_{D,j} - (1 + ds) \cdot W_j^{s} \end{cases} \tag{6}$$

3) Generation power limits:

$$P_{i,\min} \le P_{i,j}^{s} \le P_{i,\max} \tag{7}$$

4) Minimum up/down time limits:

$$\begin{cases} TON_{i,j} \ge MUT_i \\ TOFF_{i,j} \ge MDT_i \end{cases} \tag{8}$$

5) Unit ramp-up/down capacity limits:

$$-DR_i \le P_{i,j}^{s} - P_{i,j-1}^{s} \le UR_i \tag{9}$$

3. Determination of the unit scheduling solution

The procedures for determining unit scheduling solution can be described as follows.

Step 1: Assume that the probability density function (PDF) of wind power prediction error is normal distribution, and the wind power scenario set $\boldsymbol{X}_M$ can be generated by Latin hypercube sampling (LHS) [19] with Cholesky decomposition (CD) [20].

$$\begin{aligned} &\boldsymbol{X}_M = \{X_m\} \quad m = 1, 2, \cdots, M \\ &X_m = [W_1^m, W_2^m, \cdots, W_T^m] \end{aligned}, \tag{10}$$

where the wind power output can be expressed as

$$\begin{aligned} &W_j^m = \hat{W}_j + \Delta W_j^m, \Delta W_j^m \sim N(0, \delta_{w,j}^2) \\ &j = 1, 2, \cdots, T;\ m = 1, 2, \cdots, M \end{aligned} \tag{11}$$

Step 2: Calculate priority list for the thermal units:

$$\pi_i = \omega_1 \times \frac{P_{i,\max}}{\sum_{i=1}^{N} P_{i,\max}} + \omega_2 \times \frac{1/(f_i(P_{i,\max})/P_{i,\max})}{\sum_{i=1}^{N} 1/(f_i(P_{i,\max})/P_{i,\max})}, \tag{12}$$

where ω_1 and ω_2 are weight coefficients and f_i represents the fuel cost function of unit i.

Step 3: Set $m = 1$.

Step 4: Define the agent U_m as the unit scheduling solution for X_m.

$$U_m = \begin{bmatrix} u_{1,1}^m & u_{1,2}^m & \cdots & u_{1,T}^m \\ u_{2,1}^m & u_{2,2}^m & \cdots & u_{2,T}^m \\ \vdots & \vdots & \vdots & \vdots \\ u_{N,1}^m & u_{N,2}^m & \cdots & u_{N,T}^m \end{bmatrix}, \tag{13}$$

where the element values in U_m represent the units' on/off status and are set to 0.

Step 5: Modify the element values in U_m according to system spinning reserve and the minimum up/down time limits.

Step 6: Shut down the excess units in U_m, according to [21].

Step 7: For scenario X_m, the satisfying unit scheduling solution U_m can be obtained.

Step 8: If $m <$ M, then $m = m+1$ and return to Step 4; otherwise, go to Step 9.

Step 9: Generate the probability matrix P_{uc} with Eq. (14), the elements of which can be calculated by Eq. (15).

$$P_{uc} = \begin{bmatrix} p_{1,1} & p_{1,2} & \cdots & p_{1,T} \\ p_{2,1} & p_{2,2} & \cdots & p_{2,T} \\ \vdots & \vdots & \vdots & \vdots \\ p_{N,1} & p_{N,2} & \cdots & p_{N,T} \end{bmatrix} \tag{14}$$

$$p_{i,j} = \frac{1}{M} \sum_{m=1}^{M} u_{i,j}^{m} \tag{15}$$

Step 10: The final unit scheduling solution for the scenario set $\boldsymbol{X}_M$ is defined as U_R by Eq. (16), whose elements can be obtained by Eq. (17). In addition, the elements in U_R should satisfy the minimum up/down time constraints.

$$U_R = \begin{bmatrix} u_{1,1} & u_{1,2} & \cdots & u_{1,T} \\ u_{2,1} & u_{2,2} & \cdots & u_{2,T} \\ \vdots & \vdots & \vdots & \vdots \\ u_{N,1} & u_{N,2} & \cdots & u_{N,T} \end{bmatrix} \tag{16}$$

$$u_{i,j} = \begin{cases} 1 & \text{if } p_{i,j} \geq \alpha \\ 0 & \text{otherwise} \end{cases}, \tag{17}$$

where α denotes a predefined significance level.

4. Enhanced multiobjective particle swarm optimization

4.1. Overview of multiobjective particle swarm optimization

Particle swarm optimization (PSO) is a heuristic intelligent optimization algorithm [22]. During the optimization process, all particles update their positions in the feasible space according to their own experience and social information in pursuit of the optimal solution. The main improvements of MOPSO are described in the following section.

4.1.1. Establishment of external repository

Create external repository composed of a number of elites [12], which can be represented as $\boldsymbol{R}_l$, $l = 1, 2, \ldots,$ *rep*, and *rep* is the number of elites. The individual $\boldsymbol{P}_i$ can be deposited into the repository if, and only if:

$$\forall j \in [1, 2, \cdots, pop] \wedge j \neq i, \ \ \neg\exists P_i \in \Omega : P_j \prec P_i \tag{18}$$

4.1.2. Selection of the global best position

A variation in the adaptive grid is used to generate uniformly distributed Pareto front. In this way, each elite in the external repository is assigned a grid index, and the elites with the same grid index form a group and

are assigned the same fitness value. Then a randomly selected elite from the chosen group is regarded as the global best position.

4.2. Enhanced MOPSO for DEED

4.2.1. Structure of individuals

In this study, the simultaneous backward reduction technique [23] is implemented to obtain the reduced set $\{X_s\}$. For the scenario X_s, the individual $\boldsymbol{P}_i$ can be defined as

$$\boldsymbol{P}_i = \begin{bmatrix} P^s_{1,1} & P^s_{1,2} & \cdots & P^s_{1,T} \\ P^s_{2,1} & P^s_{2,2} & \cdots & P^s_{2,T} \\ \vdots & \vdots & \vdots & \vdots \\ P^s_{N,1} & P^s_{N,2} & \cdots & P^s_{N,T} \end{bmatrix}, \quad i = 1, 2, \cdots, pop \tag{19}$$

4.2.2. Dual population evolution mechanism

The initial population can be divided into main population and secondary population. For the main population, the selection of the best individual is detailed in [12]. In contrast, a unique selection and combination strategy is proposed to choose the best individual for the secondary population. The best individual and elites for the secondary population are defined as $\dot{\boldsymbol{P}}_g$ and $\dot{\boldsymbol{R}}_l$, respectively, and $\dot{\boldsymbol{R}}_l$ can be expressed as

$$\dot{R}_l = \begin{bmatrix} P^s_{1,1} & P^s_{1,2} & \cdots & P^s_{1,T} \\ P^s_{2,1} & P^s_{2,2} & \cdots & P^s_{2,T} \\ \vdots & \vdots & \vdots & \vdots \\ P^s_{N,1} & P^s_{N,2} & \cdots & P^s_{N,T} \end{bmatrix} = [P^s_{l,1}, P^s_{l,2}, \cdots, P^s_{l,T}] \tag{20}$$
$$P^s_{l,j} = [P^s_{1,j}, P^s_{2,j}, \cdots, P^s_{N,j}]^T; l = 1, 2, \cdots, rep;\ j = 1, 2, \cdots, T$$

The diagram of the selection and combination strategy is shown in Figure 1. As is shown, $\dot{\boldsymbol{P}}_g$ consists of T column vectors, which are selected from the corresponding column vectors of $\dot{\boldsymbol{R}}_l$. For each selection process, the equiprobable roulette wheel selection strategy is adopted to choose an elite.

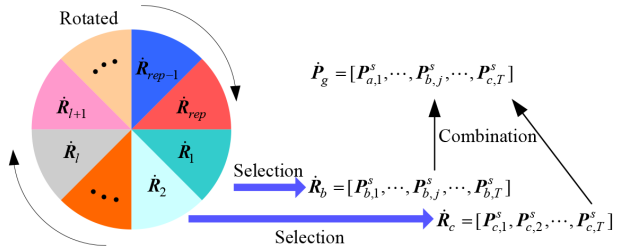

Figure 1. Schematic diagram of the selection and combination strategy.

4.2.3. Elitism-preserving strategy based on crowding entropy

A new elitism-preserving strategy is used to uniformly distribute the Pareto optimal solutions in the objective function space.

Combined with the crowding distance and distribution entropy, the crowding entropy (CE) is presented to measure the crowding degree of the solutions in the objective function space [24]. The crowding entropy of elite l can be defined as CE_l, the calculation procedure of which is detailed in [24]. The elites with objective function extrema are retained. The elites with smaller CE_l will be removed if the repository size is larger than *rep*.

5. Implementation of EMOPSO for solving DEED

5.1. Initialization

Based on the unit scheduling solution U_R determined in Section 3, the elements in $\mathbf{P}_i$ can be initialized as follows:

$$P_{i,j}^{s} = u_{i,j} \cdot (P_{i,j}^{s,\min} + rand \cdot (P_{i,j}^{s,\max} - P_{i,j}^{s,\min})), \tag{21}$$

where *rand* is random value uniformly distributed within a range from 0 to 1.

For scenario s, the generation output limits of unit i at hour j can be obtained by

$$\begin{cases} P_{i,j}^{s,\max} = \min\{P_{i,\max}, P_{i,j-1}^{s} + UR_i\} \\ P_{i,j}^{s,\min} = \max\{P_{i,\min}, P_{i,j-1}^{s} - DR_i\} \end{cases} \tag{22}$$

The generation power limits and ramp-up/down limits before hour j can be satisfied by Eq. (22). However, the time periods after hour j may have an impact on $P_{i,j}^{s}$, which can be illustrated in Figure 2.

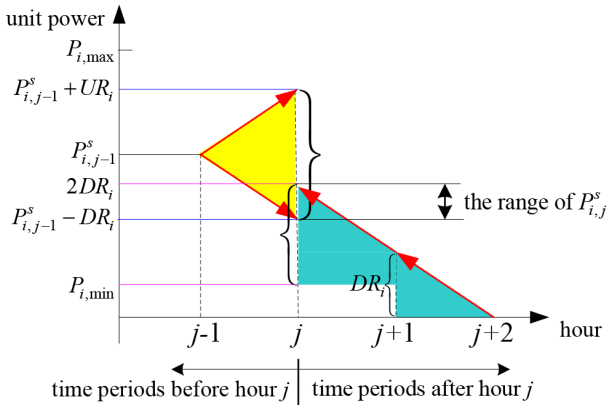

Figure 2. Diagram of generation output limits of unit i at hour j.

As shown in Figure 2, assume that the status of unit i at hour $j+2$ is off; then $P_{i,j+2}^{s}$ is 0. As a result, the value of $P_{i,j+1}^{s}$ cannot exceed DR_i, considering the ramp-down rate limit. Furthermore, the range of $P_{i,j}^{s}$ should be limited between $P_{i,\min}$ and $2DR_i$, taking into account the influence of the time periods after hour j. Combined with the generation output limits in Eq. (22), the value of $P_{i,j}^{s,\max}$ should be modified as follows:

$$P_{i,j}^{s,\max} = \min\{P_{i,\max}, P_{i,j-1}^{s} + UR_i, (j_{stop} - j) \cdot DR_i\}, \tag{23}$$

where j_{stop} denotes the first time that the status of unit i is off after hour j.

Then adjust the power output of the thermal units to meet system power balance constraints, according to [25].

5.2. Calculation of the objective and violation function values

The cost and emission values of the individual can be obtained by Eqs. (1)–(4), and the violation function value can be calculated by

$$f_{viol}^{s} = \sum_{j=1}^{T} \left| P_{D,j} - \sum_{i=1}^{N} u_{i,j} \cdot P_{i,j}^{s} - W_{j}^{s} \right| \tag{24}$$

5.3. Establishment of external repositories

Two different external repositories, noted as $\{\boldsymbol{R}_l\}$ and $\{\dot{\boldsymbol{P}}_l\}$, are established for the main population and the secondary population, respectively.

5.4. Main loop of EMOPSO for solving the DEED problem

1. Set the iteration $gen = 1$.
2. Select $\boldsymbol{R}_g$ from $\{\boldsymbol{R}_l\}$ according to the principle described in Section 4.1.2.
3. Update and mutate the individuals of the main population.
4. Select $\dot{\boldsymbol{P}}_g$ from $\{\dot{\boldsymbol{R}}_l\}$ according to the proposed selection and combination strategy.
5. Update and mutate the individuals of the secondary population.
6. Update the elite sets $\{\dot{\boldsymbol{R}}_l\}$ and $\{\boldsymbol{R}_l\}$ and control their size with the elitism-preserving strategy based on CE, if necessary.
7. Set $gen = gen + 1$. If $gen_{<} MaxG$, return to 2; otherwise the main loop is finished.

The flowchart of EMOPSO for DEED is shown in Figure 3.

6. Numerical simulation

This study has chosen a thermal wind system composed of 10 thermal units and a wind farm for validation. The scheduling period is one day with 24 intervals. The detailed unit parameters, load demand, and forecasted wind power can be seen in [18]. The standard deviation (Std) $\delta_{w,j}$ of wind power prediction error is set to 20% of the prediction at hour j. The demand factors ds, us, and η are assigned 20%, 20%, and 10%, respectively.

Initially, 1000 wind power scenarios ($M = 1000$) are generated by LHS-CD. Then the reduced set, composed of 10 scenarios, can be obtained as shown in Figure 4, and the corresponding occurrence probabilities are listed in Table 1. The significance level $\alpha$is set to 0.05, 0.1, and 0.15. The unit scheduling solution under different significance levels can be obtained with the procedures for determining U_R.

Table 1. Occurrence probabilities of 10 scenarios.

Scenario	1	2	3	4	5
$Pr(s)$	0.138	0.111	0.125	0.079	0.114
Scenario	6	7	8	9	10
$Pr(s)$	0.081	0.074	0.048	0.116	0.114

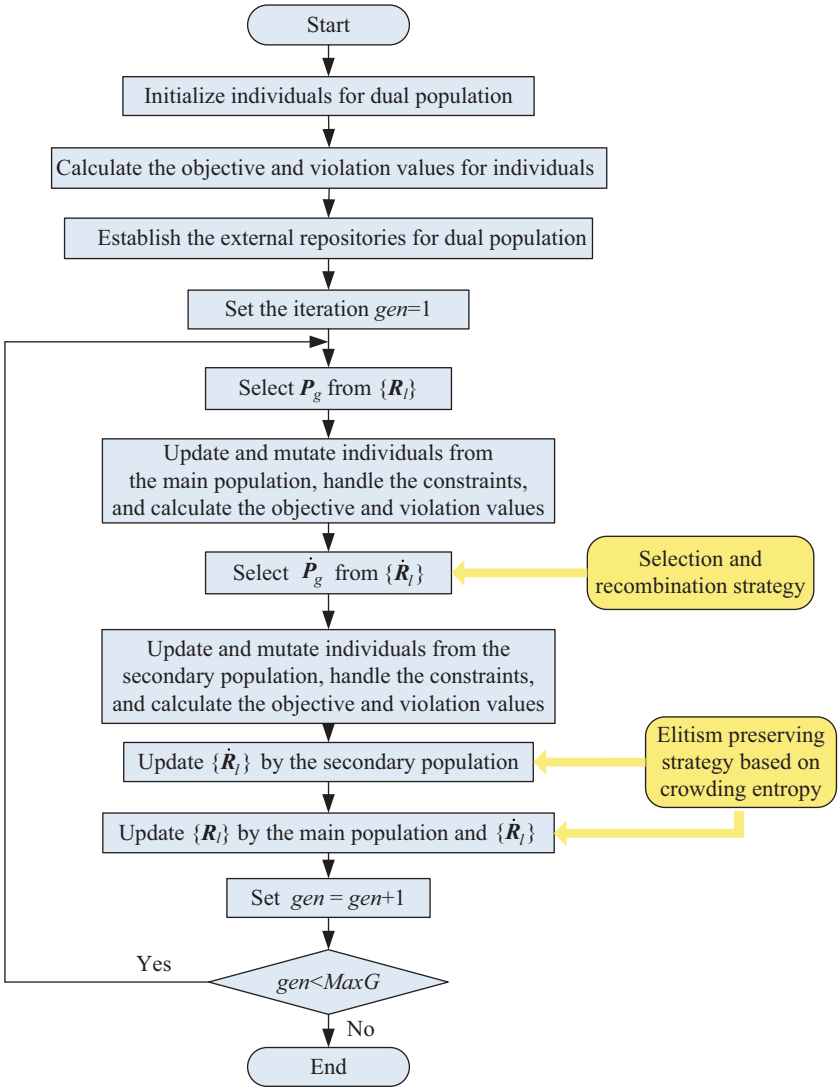

Figure 3. Flowchart of EMOPSO for DEED.

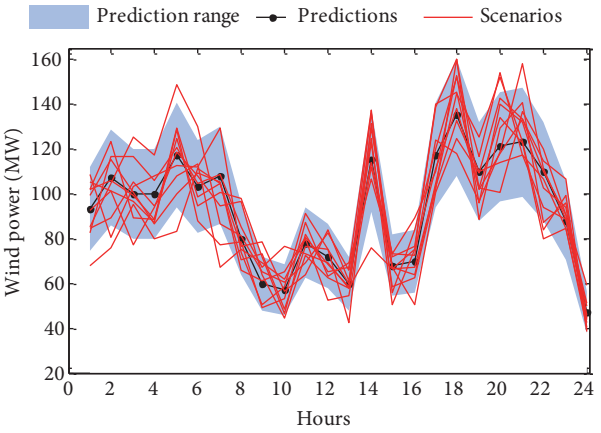

Figure 4. Reduced scenario set of wind power generation.

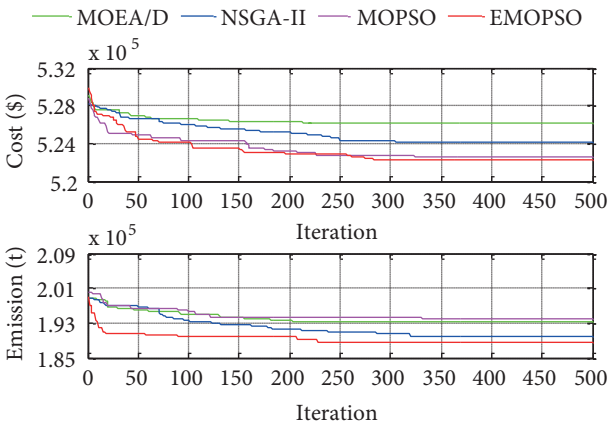

Figure 5. Convergence property of different algorithms.

In this study, several previously reported multiobjective optimization algorithms that contain NSGA-II, MOPSO, and MOEA/D have been chosen for comparison. The number of individuals and the size of the external repository are set to 60 and 30, respectively. The maximum number of iterations for all the algorithms is set to 500. When the significance level α is 0.05, the convergence property of different algorithms for Scenario 1 can be seen in Figure 5. It is shown that the objective function values tend to show no improvement when it reaches 350 iterations. Consequently, the maximum number of iterations is set to 350 in our study.

The Pareto fronts (PFs) for Scenario 1, generated by the above algorithms when α is 0.05, are shown in Figure 6, and the corresponding cost and emission values are listed in Table 2. It has been found that: (1) the Pareto optimal solutions obtained by EMOPSO can dominate those generated by other algorithms; (2) the PFs by MOEA/D, NSGA-II, and MOPSO partially overlap; (3) EMOPSO achieved the largest scope in objective function space, whereas MOEA/D obtained the smallest range; (4) compared to MOPSO, EMOPSO can obtain superior Pareto optimal solutions. The reason is that the introduced secondary population follows a unique updating strategy for the global optimal position, which is conducive to improving population diversity and enhancing search ability. Moreover, the PF by EMOPSO shows more uniform distribution in the objective function space, which demonstrates that the elitism-preserving strategy based on CE can optimize the distribution of the solutions.

Table 2. Comparison of cost and emission by different algorithms for Scenario 1.

Algorithms	Best compromise		Minimum cost		Minimum emission	
	Cost ($)	Emission (t)	Cost ($)	Emission (t)	Cost ($)	Emission (t)
MOEA/D	528,482	204,433	526,642	211,612	531,997	193,996
NSGA-II	529,144	203,871	524,671	229,437	533,352	191,069
MOPSO	528,847	203,513	522,724	235,073	532,489	194,982
EMOPSO	528,048	200,689	522,591	233,596	533,025	189,583

Regarding the best compromise solution by EMOPSO in Scenario 1, when α is 0.05, the power outputs of the thermal units that meet the operation constraints of the units are shown in Figure 7. To test the stability of EMOPSO, this study performed the simulation 20 times, and the best compromise solutions in the 20 trials are shown in Figure 8. Additionally, the best, worst, average, and Std values of cost and emission are listed in Table 3, which shows that the cost and emission of the best compromise solutions have a fluctuation in a small range.

Table 3. Statistical results for the best compromise solutions by EMOPSO.

Objective	Best	Worst	Average	Std
Cost ($)	527,668	528,341	528,008	194
Emission (t)	199,840	202,663	201,282	799

To solve the SDEED problem for the reduced scenario set by EMOPSO, the PFs under different significance levels are shown in Figure 9, and the expected values of the best compromise solutions and extreme solutions are listed in Table 4. The reserve not served (RNS) can be calculated by

$$\begin{aligned} RNS_j^s &= \begin{cases} -temp & \text{if} \quad temp < 0 \\ 0 & \text{if} \quad temp \geq 0 \end{cases}, \\ temp &= \sum_{i=1}^{N} (P_{i,j}^{s,\max} \cdot u_{i,j} - P_{i,j}^s) - \eta \cdot P_{D,j} \end{aligned} \tag{25}$$

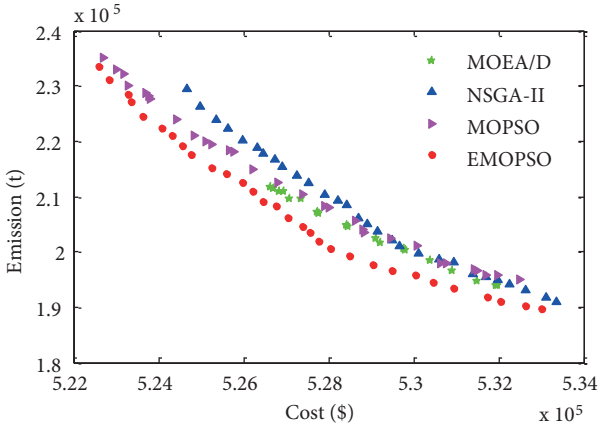

Figure 6. Pareto optimal fronts for Scenario 1 when $\alpha = 0.05$.

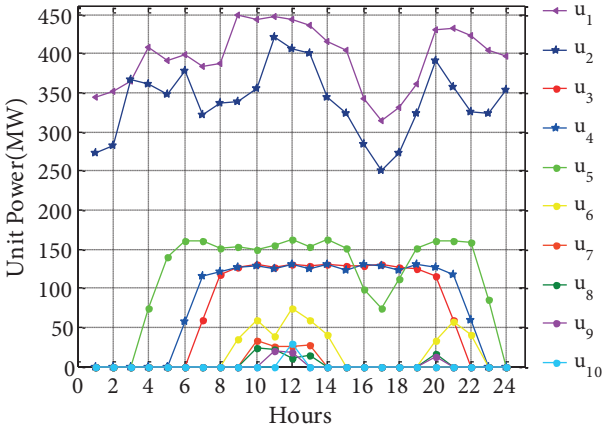

Figure 7. Power outputs by EMOPSO for Scenario 1 when $\alpha = 0.05$.

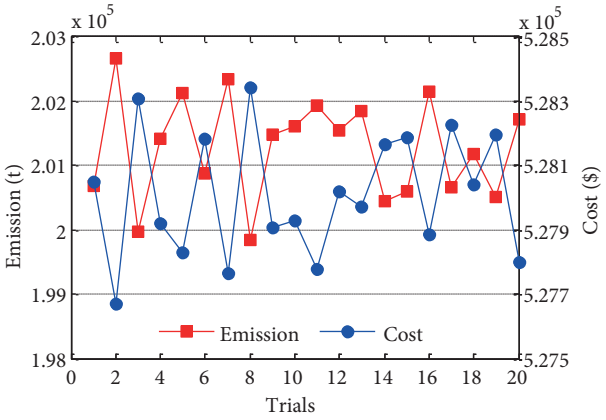

Figure 8. Best compromise solutions in 20 trials by EMOPSO.

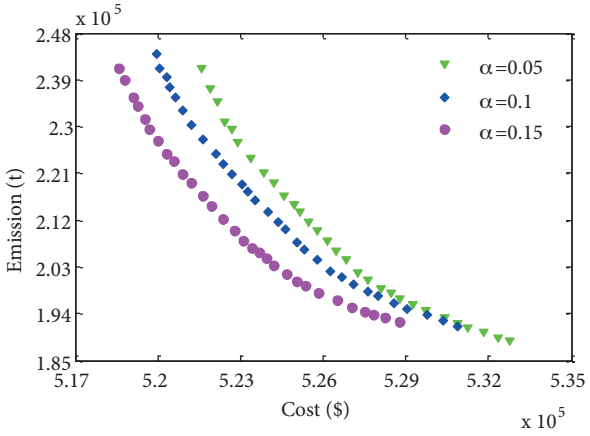

Figure 9. Pareto optimal fronts for SDEED under different significance levels.

The RNS for the reduced scenario set, under different significance levels, is illustrated in Figures 10–12.

Table 4. Comparison of the expected values of the cost and emission by EMOPSO.

Significance level	Best compromise		Minimum cost		Minimum emission	
	Cost ($)	Emission (t)	Cost ($)	Emission (t)	Cost ($)	Emission (t)
0.05	526,178	207,887	521,617	241,202	532,761	188,692
0.1	525,337	206,192	519,972	243,837	530,884	191,528
0.15	523,957	204,514	518,617	241,075	528,759	192,269

In Table 4, as the significance level α decreases, the operational reliability for the unit-scheduling solution is enhanced, and more units will be committed during the entire scheduling period. Consequently, the expected values of cost and emission for the best compromise solution have increased gradually. In contrast, as the value of α increases, the reserve not served increases prominently. Figures 10–12 show that the summation of RNS for the reduced scenario set is 30.24 MWh, 124.50 MWh, and 370.57 MWh, respectively, as α rises from 0.05 to 0.15.

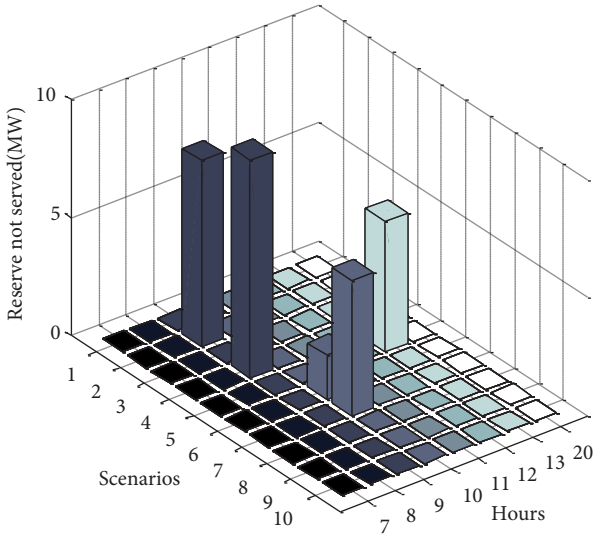

Figure 10. The reserve not served for different scenarios when $\alpha = 0.05$.

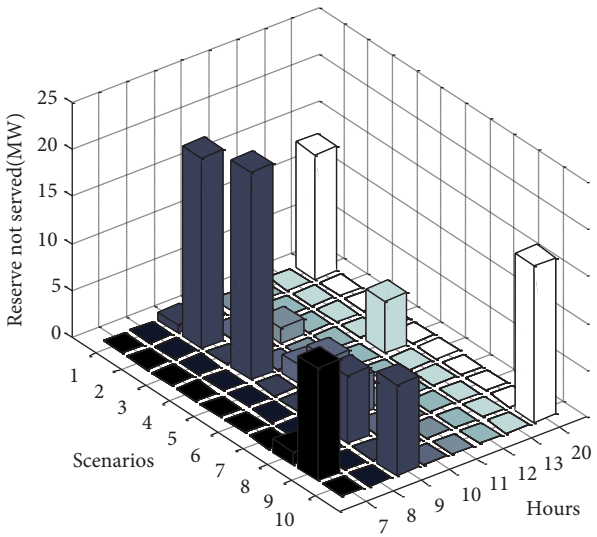

Figure 11. The reserve not served for different scenarios when $\alpha = 0.1$.

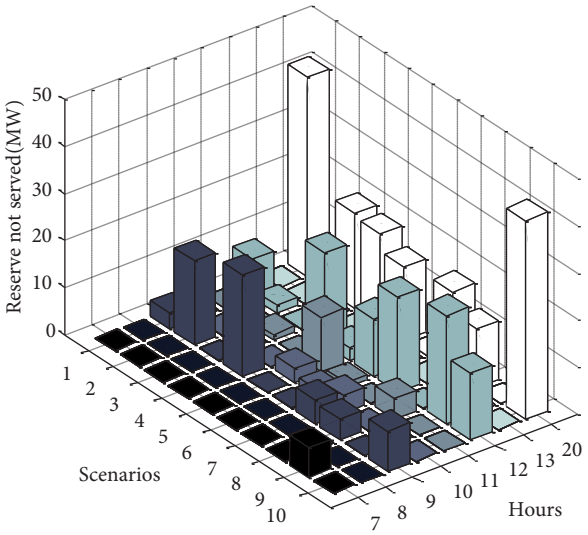

Figure 12. The reserve not served for different scenarios when $\alpha = 0.15$.

7. Conclusion

This paper established a probabilistic scenario-based framework to solve SDEED-UC integrated with wind power. The UC solution can be obtained for a predefined significance level α. Lower value of α denotes that more units will be committed during the whole scheduling period. To solve the DEED problem, the units' on/off status and the ramp up/down capacity limits were considered simultaneously. The proposed EMOPSO algorithm has great advantages over other comparison algorithms. Moreover, simulation results under different significance levels demonstrate that the expected values of cost and emission for the best compromise solution at a higher significance level are lower; however, the corresponding reserve capacity not served increased.

Nomenclature

i	thermal unit index
j	time interval index
m	original scenario index
s	reduced scenario index
N	number of thermal units
M	number of original scenarios
S	number of reduced scenarios
T	number of time intervals
$Pr(s)$	probability of scenario s
$\boldsymbol{X}_M$	original scenario set
$\hat{W}_j$	wind power prediction at hour j
ΔW_j^m	wind power forecasting error at hour j for scenario m
W_j^m	wind power output at hour j for scenario m
$P_{D,j}$	load demand at hour j
$P_{i,\max}$	maximum power output of unit i
$P_{i,\min}$	minimum power output of unit i
$P_{i,j}^{s,\max}$	maximum generation output of unit i at hour j for scenario s
$P_{i,j}^{s,\min}$	minimum generation output of unit i at hour j for scenario s
MUT_i	minimum up time of unit i
MDT_i	minimum down time of unit i
UR_i	ramp-up rate of unit i
DR_i	ramp-down rate of unit i
us	demand factor of up-spinning reserve for wind power fluctuation
ds	demand factor of down-spinning reserve for wind power fluctuation
η	demand factor of up-spinning reserve for load forecast errors
SC_i^{hot}	hot startup cost of unit i
SC_i^{cold}	cold startup cost of unit i
SC_i	startup cost of unit i
T_i^{cold}	cold startup time of unit i
$TON_{i,j}$	time period that unit i has been on until hour j
$TOFF_{i,j}$	time period that unit i has been off until hour j
$u_{i,j}$	on/off state of unit i at hour j
$P_{i,j}^s$	generation power of unit i at hour j for scenario s
RNS_j^s	reserve not served at hour j for scenario s

Acknowledgments

This work was supported by the National Natural Science Foundation of China (Project No. 51309258) and the National Basic Research Program of China (Project No. 973 Program-2012CB215101).

References

[1] Abujarad SY, Mustafa MW, Jamian JJ. Recent approaches of unit commitment in the presence of intermittent renewable energy resources: a review. Renew Sust Energ Rev 2017; 70: 215-223.

[2] Wang Y, Zhao S, Zhou Z, Botterud A, Xu Y, Chen R. Risk adjustable day-ahead unit commitment with wind power based on chance constrained goal programming. IEEE T Sustain Energ 2017; 8: 530-541.

[3] Ji B, Yuan X, Chen Z, Tian H. Improved gravitational search algorithm for unit commitment considering uncertainty of wind power. Energy 2014; 67: 52-62.

[4] Blanco I, Morales JM. An efficient robust solution to the two-stage stochastic unit commitment problem. IEEE T Power Syst 2017; 99: 1-11.

[5] Zhang H, Yue D, Xie X. Robust optimization for dynamic economic dispatch under wind power uncertainty with different levels of uncertainty budget. IEEE Access 2016; 4: 7633-7644.

[6] Zaman MF, Elsayed SM, Ray T, Sarker RA. Evolutionary algorithms for dynamic economic dispatch problems. IEEE T Power Syst 2016; 31: 1486-1495.

[7] Sonmez Y, Kahraman HT, Dosoglu MK, Guvenc U, Duman S. Symbiotic organisms search algorithm for dynamic economic dispatch with valve-point effects. J Exp Theor Artif In 2017; 29: 495-515.

[8] Jebaraj L, Venkatesan C, Soubache I, Rajan CCA. Application of differential evolution algorithm in static and dynamic economic or emission dispatch problem: a review. Renew Sust Energ Rev 2017; 77: 1206-1220.

[9] Dosoglu MK, Guvenc U, Duman S, Sonmez Y, Kahraman HT. Symbiotic organisms search optimization algorithm for economic/emission dispatch problem in power systems. Neural Comput Appl 2016: 1-17.

[10] Alham MH, Elshahed M, Ibrahim DK, Zahab EEDAE. A dynamic economic emission dispatch considering wind power uncertainty incorporating energy storage system and demand side management. Renew Energ 2016; 96: 800-811.

[11] Deb K, Pratap A, Agarwal S, Meyarivan T. A fast and elitist multiobjective genetic algorithm: NSGA-II. IEEE T Evolut Comput 2002; 6: 182-197.

[12] Coello CAC, Pulido GT, Lechuga MS. Handling multiple objectives with particle swarm optimization. IEEE T Evolut Comput 2004; 8: 256-279.

[13] Zhang Q, Li H. MOEA/D: a multiobjective evolutionary algorithm based on decomposition. IEEE T Evolut Comput 2007; 11: 712-731.

[14] Abdullah MN, Bakar AHA, Rahim NA, Mokhlis H. Modified particle swarm optimization for economic-emission load dispatch of power system operation. Turk J Elec Eng & Comp Sci 2015; 23: 2304-2318.

[15] Chen F, Zhou J, Wang C, Li C, Lu P. A modified gravitational search algorithm based on a non-dominated sorting genetic approach for hydro-thermal-wind economic emission dispatching. Energy 2017; 121: 276-291.

[16] Lin S, Liu M, Li Q, Lu W, Yan Y, Liu C. Normalised normal constraint algorithm applied to multi-objective security-constrained optimal generation dispatch of large-scale power systems with wind farms and pumped-storage hydroelectric stations. IET Gener Transm Dis 2017; 11: 1539-1548.

[17] Qu BY, Liang JJ, Zhu YS, Wang ZY, Suganthan PN. Economic emission dispatch problems with stochastic wind power using summation based multi-objective evolutionary algorithm. Inform Sci 2016; 351: 48-66.

[18] Wu X, Zhang B, Li J, Luo G, Duan Y, Wang K. Solving power system unit commitment with wind farms using multi-objective quantum-inspired binary particle swarm optimization. J Renew Sustain Ener 2013; 5: 347-355.

[19] Yu H, Chung CY, Wong KP, Lee HW, Zhang J. Probabilistic load flow evaluation with hybrid Latin hypercube sampling and Cholesky decomposition. IEEE T Power Syst 2009; 24: 661-667.

[20] Harbrecht H, Peters M, Schneider R. On the low-rank approximation by the pivoted Cholesky decomposition. Appl Numer Math 2012; 62: 428-440.

[21] Yuan X, Ji B, Zhang S, Tian H, Hou Y. A new approach for unit commitment problem via binary gravitational search algorithm. Appl Soft Comput 2014; 22: 249-260.

[22] Eberhart R, Kennedy J. A new optimizer using particle swarm theory. In: IEEE 1995 International Symposium on Micro Machine and Human Science; 4–6 October 1995; New York, NY, USA. New York, NY, USA: IEEE. pp. 39-43.

[23] Wu L, Shahidehpour M, Li T. Stochastic security-constrained unit commitment. IEEE T Power Syst 2007; 22: 800-811.

[24] Wang Y, Wu L, Yuan X. Multi-objective self-adaptive differential evolution with elitist archive and crowding entropy-based diversity measure. Soft Comput 2009; 14: 193-209.

[25] Yuan X, Tian H, Yuan Y, Huang Y, Ikram RM. An extended NSGA-III for solution multi-objective hydro-thermal-wind scheduling considering wind power cost. Energ Convers Manage 2015; 96: 568-578.